Vietnam Journal of Catalysis and Adsorption
Tạp chí xúc tác và hấp phụ Việt Nam

https://jca.edu.vn

# Adsorption of $Pb^{2+}$ ions of natural red lava rock powder in aqueous media

Nguyen Thi Nang[1], Nguyen Kim Thuy[1], Nguyen Thi Thu Ly[1], Nguyen Thi Lan Anh[2], Truong Viet Hoai[3], Nguyen Thi Hoai Phuong[1,*]

[1] *Department of Chemistry and Environment, Joint Vietnam-Russia Tropical Science and Technology Research Center, Ha Noi, Vietnam*
[2] *Viet Tri University of Industry, Phu Tho, Vietnam*
[3] *Faculty of Mechanical Engineering, Le Quy Don Technical University, Ha Noi, Vietnam*
**Email: hoaiphuong1978@gmail.com*

ARTICLE INFO

Received: 28/02/2024
Accepted: 20/4/2024
Published: 30/6/2024

*Keywords:*
Lava rock; $Pb^{2+}$; adsorption; isotherm; kinetics

ABSTRACT

Red lava rock is available in nature and is formed from volcanic eruptions. Volcanic rocks are composed of oxides of diverse metals and have considerable porosity. In this study, lava rock powder was ground to a specific size and dried to test its ability to adsorb heavy metals in water. The morphology of the stone powder was observed to show crystals of 100–300 nm in size clumping into particles of a few µm. The phase structure is mainly in the form of $Ca(Mg,Al)(Si,Al)_2O_6$; in addition, the phases $CaAl_2Si_4O_{12}.2H_2O$, $Ca_2MgSi_2O_7$, and $Ca_3MgSi_2O_8$ also exist. The material's maximum $Pb^{2+}$ ion adsorption capacity reaches 32.05 mg/g at endogenous pH. The isotherm of $Pb^{2+}$ adsorption on the material follows the Langmuir model, and the adsorption kinetics are pseudo-first-order kinetics.

## 1. Introduction

Lead (Pb) is a heavy metal element that can be found in nature or obtained via various sources, including manufacturing and transportation. Many aspects of human health, such as the neurological, cardiovascular, resistance, kidney and liver function, fertility, etc., are negatively impacted by lead poisoning [1-5]. More seriously, lead has a more substantial impact on the fetus, infants, and children, such as reduced IQ, slow fetal development, reduced learning ability, and abnormal behavior [6]. In addition, lead-polluted water sources affect biodiversity, decreasing the ability of animals and plants to grow [7]. Lead has been linked to mutations, damage, and breaks in DNA, according to recent research [8]. Pb in water has been removed using a variety of techniques, including chemical precipitation [9], ion exchange [10], biology [11], etc. Adsorption methods are commonly used with materials such as $MnO_2$ [12], graphene [13], alginate [14], chitosan [15], *etc.* Recently, natural minerals such as environmentally friendly, cheap, and simple-to-use adsorbents, including bentonite [16], montmorillonite [17], sepiolite [18], etc., have been widely researched and used for the same purpose. Red lava rock (volcanic rock or Lava honeycomb rock) is a relatively cheap rock formed by volcanic eruptions. Red lava rock has a surface with many tiny holes [19]. They are often used as aquarium water filter material, bonsai growing medium, and many plants. Lava stone's chemical composition mainly includes $SiO_2$, CaO, MgO, $Fe_xO_y$, $Al_2O_3$, $TiO_2$, and $Na_2O$ ($K_2O$), so in addition to typical applications, it can also remove heavy metal ions and organic compounds like other natural stones [19-23]. This article investigated the characteristics of powdered red lava rock, and the $Pb^{2+}$ ion adsorption process was also studied and evaluated.

https://doi.org/10.62239/jca.2024.031

## 2. Experimental

### *Chemicals*

Lead (II) Nitrate $Pb(NO_3)_2$ 99.5%, Hydrochloric Acid 37.0%, Sodium Hydroxide 98.0% were purchased from Sigma Aldrich Group.

### *Sample preparation*

Natural red lava rock with size between 1-3 mm was from StoneContact Incorporated. The red lava rock was washed by deionized water and dried at 100 °C for 6 hours. Then, the rock is crushed using a steel ball mill to a particle size about 100 µm. The rock powder sample was characterized before $Pb^{2+}$ ion adsorption.

### *Characterization of sample*

The sample phase was analyzed by an X'Pert Pro X-ray diffractometer - XRD (using a CuKα anode with a scanning rate of 5°/min, 2θ range 10 ° to 80 °). The morphology and chemical composition of the sample were observed by scanning electron microscopy (SEM) combined with energy-dispersive X-ray spectroscopy - EDX. The porosity of the sample was investigated by the Nitrogen gas adsorption isotherm - BET at 77 K.

### *Removal of ion $Pb^{2+}$*

The experiments were conducted with the ratio of rock powder to the amount of $Pb^{2+}$ solution of 0.25 g/L. The sample and the $Pb^{2+}$ solution were put into a dark glass vase. In the experiments, the solution was filtered from the rock powder sample after 24 hours of adsorption and tested for $Pb^{2+}$ concentration using the Inductively Coupled Plasma (ICP) technique.

*Effect of solution pH:* Herein, 25 mg of rock powder sample was added to 100 mL of 50 ppm $Pb^{2+}$ at various pH values ranging from 3 to 11 (adjusted by 0.1 M HCl and 0.1 M NaOH solutions). The suspensions were shaken at a speed of 160 rpm at ambient temperature for 24 hours. After filtering each sample, the amount of $Pb^{2+}$ remaining was determined.

*Adsorption kinetics*: A standard experiment involved mixing 100 mL of 30 ppm $Pb^{2+}$ with 25 mg of red lava rock powder adsorbent in a glass vessel. The combined solution was agitated at 160 rpm using an orbital shaker. The mixture was filtered, and $Pb^{2+}$ was measured at predetermined intervals. First- and second-order kinetic models were used to investigate the material's adsorption kinetics.

*Adsorption isotherm*: 100 mL of $Pb^{2+}$ solution with starting concentrations ranging from 10 to 50 ppm was mixed with 25 mg of rock powder in glass jars. The adsorption process was run for 24 hours at room temperature with 160 rpm shaking. The mixes underwent filtration, and inductively coupled plasma spectrometry (ICP) was utilized to assess any remaining $Pb^{2+}$. The interaction between the adsorbent and adsorbate was investigated using the Langmuir, Freunlich, and Temkin isotherm equations.

## 3. Results and discussion

### *Characterization of red lava rock*

Red lava rock's phases were described using XRD (Figure 1a). The diffraction peaks of 20.04°, 27.70°, 29.87°, 35.06°, and 35.72° that are characteristic of the red lava rock can be attributed to the aluminosilicate $Ca(Mg,Al)(Si,Al)_2O_6$ (PDF 00-041-1370) [24,25]. Moreover, the broader diffraction peaks at 15.94°, 26.15°, and 30.88° attributed to the wairakite $CaAl_2Si_4O_{12}.2H_2O$[26]. Meanwhile, those appearing at 31.94° and 33.28° can be attributed to akermanite $Ca_2MgSi_2O_7$ and merwinite $Ca_3MgSi_2O_8$, respectively[27].

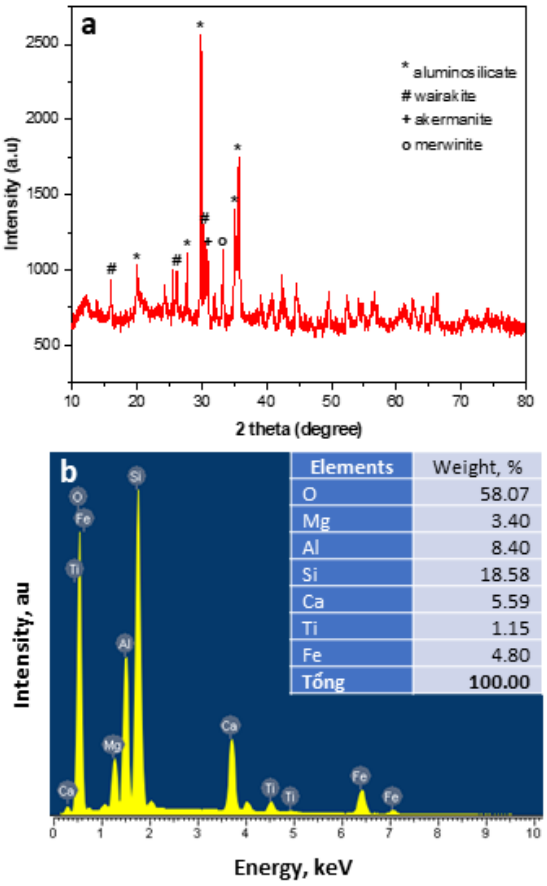


Fig. 1: XRD (a) and EDX (b) patterns of rad lava rock powder

The results of EDX analysis (Figure 1b) indicated that the sample included certain amounts of Si, Al, Ca, Mg, Fe,

and Ti. In addition, oxygen was observed in the XRD pattern. The mass of the elements proves the existence of compounds that are oxides of metals, in which Si and Al predominate. The presence of the component Fe in the sample differentiates red lava from other volcanic rocks. The representation of elemental composition from EDX also supports the representation of the structural phase in the XRD diagram.

Scanning electron microscopy was used to examine the surface morphology of red lava rock powder; the outcome is displayed in Figure 2a. The material takes the shape of 100–300 nm-diameter nanoparticles. Larger particles, ranging in size from 1 to 3 µm, are formed when nanoparticles group together.

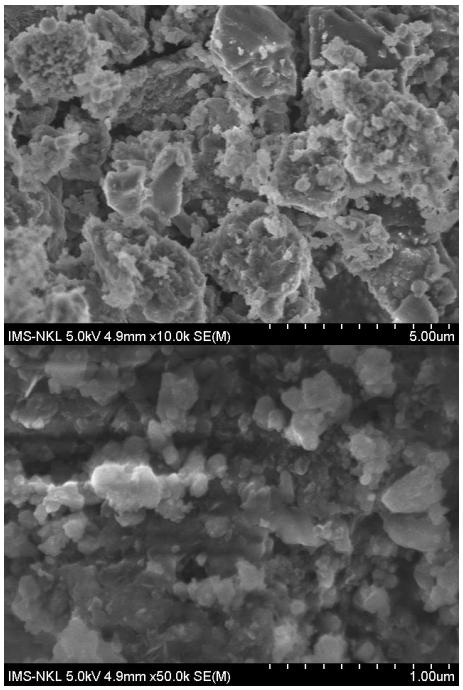


(a)

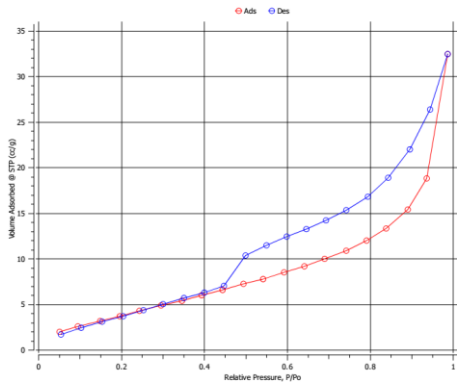


(b)

Fig. 2: SEM images (a) and $N_2$ adsorption isotherm digram (b) of red lava rock powder

Figure 2b shows the red lava rock powder's $N_2$ adsorption isotherm. The sample's BET surface area was calculated to be 17.72 $m^2/g$. Using the BJH method, the pore size and pore volume were determined to be 1.89 nm and 0.048 $cm^3/g$, respectively.

### *Effect of pH on $Pb^{2+}$ adsorption*

Figure 3 illustrates how the pH of the solution, affects the amount of $Pb^{2+}$ adsorbed by the red lava rock. It is clear that the pH of the solution significantly impacted $Pb^{2+}$'s ability to adsorb. $Pb^{2+}$ adsorption in acidic conditions increased gradually as the pH of the solution rose, reaching a maximum adsorption capacity range of 31.30–42.18 mg/g at a pH range of 3–7. The adsorption capacity rose as the pH of the solution was raised even higher. Precipitation will not happen at pH ≤ 8 according to the precipitation constant, $K = 1.2 \times 10^{-15}$, and the starting $Pb^{2+}$ concentration in this investigation, C = 50 ppm[28].

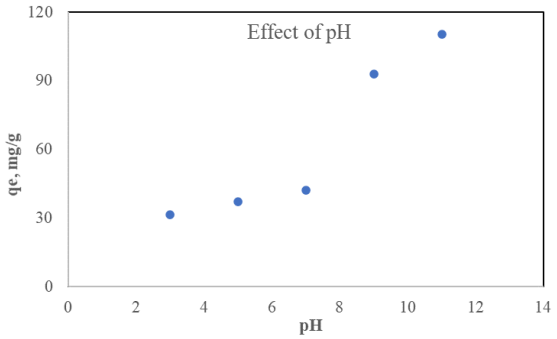


Fig. 3: Effect of solution pH on $Pb^{2+}$ adsorption by red lava rock powder

### *Adsorption kinetics and isotherm*

The Langmuir, Freundlich, and Temkin models were employed to explain the $Pb^{2+}$ adsorption isotherms on the powdered red lava rock. According to the Langmuir isotherm model, metal ion absorption occurs on a uniform material surface. There is no interaction between the adsorbed ions, and the adsorption is monolayer within the investigated range. The following formula provides the Langmuir isotherm model's linear equation:

$$\frac{C_e}{q_e} = \frac{C_e}{q_m} + \frac{1}{K_L q_m} \quad (1)$$

The Freundlich isotherm model is an empirical equation based on adsorption on heterogeneous material surfaces. Often, the linear equation is shown as:

$$lnq_e = lnK_F + \frac{1}{n} lnC_e \quad (2)$$

According to the Tempkin isotherm model, covering density causes a linear decrease in the amount of heat absorbed by each molecule on the material surface. This results from the interaction between the adsorbent and

the adsorbent, where adsorption is characterized by a uniform distribution of binding energies and a maximal binding energy. The Temkin isotherm is represented by the equation that follows:

$$q_e = BlnC_e + BlnA \quad (3)$$

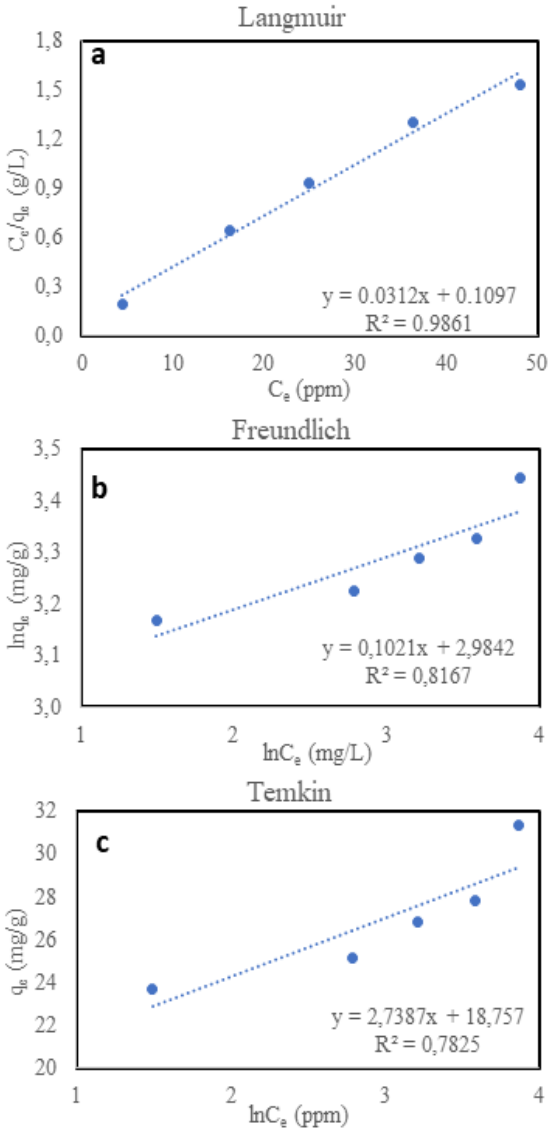


Fig. 4: The linear plot of isotherm data based on Langmuir (a), Freundlich (b), and Temkin (c) models

Figures 4a, b, and c, respectively, display the linear plots of experimental data based on the Langmuir, Freundlich, and Temkin models. With a regression coefficient of $R^2$ = 0.9861, the Langmuir model fits the data better than the Freundlich model ($R^2$ = 0.8167) and the Temkin model ($R^2$ = 0.7825). The sample's maximum adsorption capacity, as determined by the Langmuir model, is 32.05 mg/g. The surface area and porosity of lava rock may play a role in its adsorption capacity towards $Pb^{2+}$. This suggests that the $Pb^{2+}$ ions are adsorbed on lava rock powder as a monolayer.

Table 1: The isotherm parameters for $Pb^{2+}$ adsorption by the red lava rock powder

| Isotherm model | Parameters |
|---|---|
| Langmuir | $K_L$ (L/mg) = 0.2844<br>$q_{max}$ (mg/g) = 32.05<br>$R^2$ = 0.9861 |
| Freundlich | $K_F$ (mg/g)(L/mg)$^{1/n}$ = 19.77<br>n = 9.794<br>$R^2$ = 0.8167 |
| Temkin | A (L/g) = 0.942<br>B = 2.7387<br>$b_T$ (kJ/mol) = 0.8288<br>$R^2$ = 0.7825 |

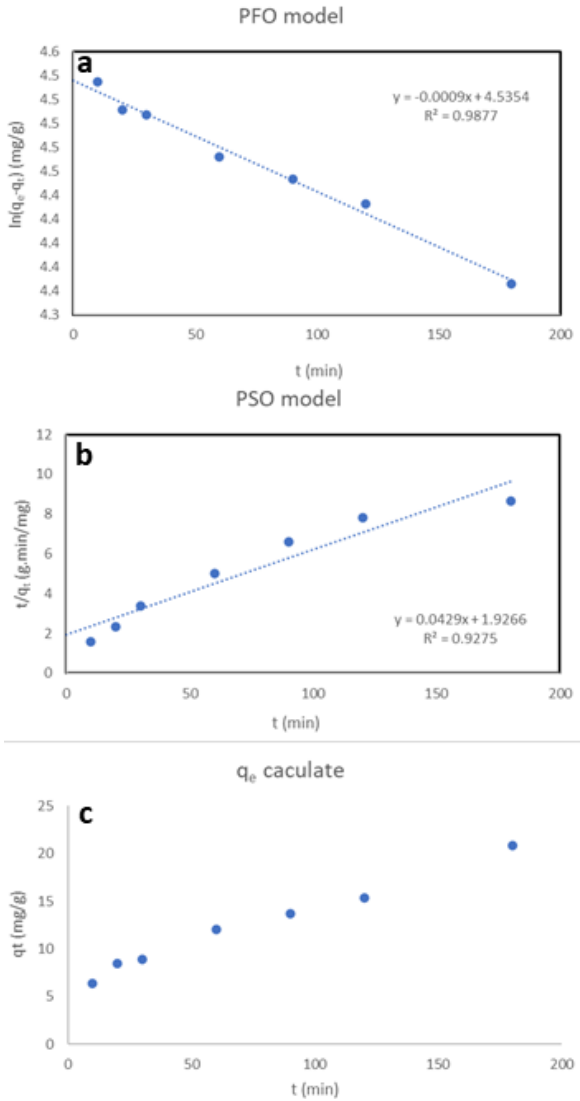


Fig. 5: Pseudo–first–order (a), pseudo–second–order kinetics (b), and pseudo-second-order kinetic model (c) for the $Pb^{2+}$ elimination process.

The mechanism of heavy metal adsorption and possible rate-control processes on the adsorbent can be examined using the adsorption kinetics. The pseudo-

first-order and pseudo-second-order kinetic models were fitted to the experimental data of adsorption. These models' linear form is provided as follows:

$$\log(q_e - q_t) = log q_e - \frac{k_1 t}{2.303} \quad (4)$$

$$\frac{t}{q_t} = \frac{1}{k_2 q_e^2} + \frac{t}{q_e} \quad (5)$$

where $q_e$ and $q_t$ (mg/g) represent the amounts of adsorption at equilibrium and at time t, respectively; $k_1$ (L/min) and $k_2$ (mg/g·min) are the rate constants of pseudo-first-order and pseudo-second-order adsorption, respectively.

The linearized plots of the examined kinetic models are shown in Figure 5. The finding show that the pseudo-first-order kinetic model with $R^2$ = 0.9877 best describes the $Pb^{2+}$ adsorption onto red lava rock powder.

## 4. Conclusion

According to the study's findings, red lava rock powder that is readily available can absorb heavy metals from contaminated water. After grinding and drying, stone powder has a morphology of crystals of several hundred nm clustered into larger particles of several um in size. The phase structure is mainly aluminosilicate, but wairakite, akermanite, and merwinite phases also exist. The rock's elemental composition includes Si, Al, Ca, Mg, Fe, and Ti. Lava rock powder adsorbs $Pb^{2+}$ ions with a maximum 32.05 mg/g capacity at endogenous pH. $Pb^{2+}$ adsorption isotherm on the material is in accordance with the Langmuir model, and pseudo-first-order adsorption kinetics are observed. The foundation for promising material found in nature is the data gathered from the survey.

## Acknowledgments

This research is funded by Department of Chemistry and Environment, Joint Vietnam-Russia Tropical Science and Technology Research Center.

## References

1. M.S. Collin, S.K. Venkatraman, N. Vijayakumar, V. Kanimozhi, S.M. Arbaaz, R.G.S. Stacey, J. Anusha, R. Choudhary, V. Lvov, G.I. Tovar, F. Senatov, S. Koppala, S. Swamiappan, Journal of Hazardous Materials Advances 7 (2022) 100094. https://doi.org/10.1016/j.hazadv.2022.100094
2. M. Boskabady, N. Marefati, T. Farkhondeh, F. Shakeri, A. Farshbaf, M.H. Boskabady, Environ Int 120 (2018) 404-420. https://doi.org/10.1016/j.envint.2018.08.013
3. C. Giulioni, V. Maurizi, V. De Stefano, G. Polisini, J.Y. Teoh, G. Milanese, A.B. Galosi, D. Castellani, Reprod Toxicol 118 (2023) 108387. https://doi.org/10.1016/j.reprotox.2023.108387
4. C. Niu, M. Dong, Y. Niu, Phytomedicine 114 (2023) 154789. https://doi.org/10.1016/j.phymed.2023.154789
5. K. Raj, A.P. Das, Environmental Chemistry and Ecotoxicology 5 (2023) 79-85. https://doi.org/10.1016/j.enceco.2023.02.001
6. V.I. Naranjo, M. Hendricks, K.S. Jones, Pediatr Neurol 113 (2020) 51-55. https://doi.org/10.1016/j.pediatrneurol.2020.08.005
7. S.U. Rahman, J.C. Han, M. Ahmad, S. Gao, K.A. Khan, B. Li, Y. Zhou, X. Zhao, Y. Huang, Sci Total Environ 904 (2023) 166677. https://doi.org/10.1016/j.scitotenv.2023.166677
8. S. Hemmaphan, N.K. Bordeerat, Int J Environ Res Public Health 19 (2022). https://doi.org/10.3390/ijerph19074307
9. W. Bai, R. Tang, G. Wu, W. Wang, S. Yuan, L. Xiao, X. Zhan, Z.H. Hu, J Hazard Mater 455 (2023) 131633. https://doi.org/10.1016/j.jhazmat.2023.131633
10. H. Mekatel, S. Amokrane, A. Benturki, D. Nibou, Procedia Engineering 33 (2012) 52-57. https://doi.org/10.1016/j.proeng.2012.01.1176
11. J. Wu, T. Wang, J. Wang, Y. Zhang, W.P. Pan, Sci Total Environ 754 (2021) 142150. 10.1016/j.scitotenv.2020.142150
12. H. Gong, Y. Cao, W. Zeng, C. Sun, Y. Wang, J. Su, H. Ren, P. Wang, L. Zhou, G. Kai, J. Qian, Environmental Research (2024). https://doi.org/10.1016/j.envres.2024.118360
13. Z. Mei, L. Bo, C. Yanguang, Z. Jiaojing, Z. Yanan, S. Hua, H. Soleymanabadi, J. Wu, Journal of Industrial and Engineering Chemistry (2023). https://doi.org/10.1016/j.jiec.2023.11.052
14. L. Xu, T. Bai, X. Yi, K. Zhao, W. Shi, F. Dai, J. Wei, J. Wang, C. Shi, Int J Biol Macromol 238 (2023) 124131. https://doi.org/10.1016/j.ijbiomac.2023.124131
15. M.B. Yahia, R. Gerhardt, L. Sellaoui, H.Y.S. Al-Zahrani, A.P.O. Inácio, D. Dias, T.R.S.A. Cadaval, L.A. de Almeida Pinto, A. Bonilla-Petriciolet, M. Badawi, Separation and Purification Technology 337 (2024). https://doi.org/10.1016/j.seppur.2024.126451
16. A.L. Obsa, N.T. Shibeshi, E. Mulugeta, G.A. Workeneh, Results in Engineering 21 (2024). https://doi.org/10.1016/j.rineng.2024.101756
17. J. Du, A. Zhou, X. Lin, Y. Bu, Environ Res 209 (2022) 112817. 10.1016/j.envres.2022.112817
18. Y. Gu, H. Feng, B. Wang, J. Qiu, X. Meng, L. Zhang, B. Zhang, N. Chen, L. Tan, Microporous and Mesoporous Materials 363 (2024). https://doi.org/10.1016/j.micromeso.2023.112821
19. B. Song, Z. Wang, J. Li, M. Luo, P. Cao, C. Zhang, Chemical Engineering Journal 426 (2021). 10.1016/j.cej.2021.131940
20. G. Zhang, W. Chen, M. Dou, D. Su, J. Zhang, Z. Zhao, Renewable Energy 217 (2023). https://doi.org/10.1016/j.renene.2023.119214
21. X. Zhu, T. Song, Z. Lv, G. Ji, Process Safety and Environmental Protection 104 (2016) 373-381. https://doi.org/10.1016/j.psep.2016.09.019
22. H.-h. Ji, F.-x. Ling, P. Wang, B.-k. Sui, S.-j. Wang, S.-h. Yuan, Journal of Fuel Chemistry and Technology 49 (2021) 1049-1056. https://doi.org/10.1016/s1872-5813(21)60107-x
23. E. Alemayehu, B. Lennartz, J Hazard Mater 169 (2009) 395-401. https://doi.org/10.1016/j.jhazmat.2009.03.109
24. R.P. Wilkerson, M.P. Petkov, G.E. Voecks, C.S. Lynch, H.S. Shulman, S. Sundaramoorthy, A. Choudhury, D.L. Rickman, M.R. Effinger, Icarus 400 (2023). https://doi.org/10.1016/j.icarus.2023.115577

25. M. Liu, A. Iizuka, E. Shibata, Materials Transactions 60 (2019) 61-67. https://doi.org/10.2320/matertrans.M-M2018848
26. S. Ori, S. Quartieri, G. Vezzalini, V. Dmitriev, American Mineralogist 93 (2008) 53-62. 10.2138/am.2008.2554
27. R. Choudhary, S. Koppala, S. Swamiappan, Journal of Asian Ceramic Societies 3 (2018) 173-177. https://doi.org/10.1016/j.jascer.2015.01.002
28. X. Di, T. Xiaoli, C. Changlun, W. Xiangke, Journal of Hazardous Materials 154 (2008) 407-423. http://dx.doi.org/10.1016/j.jhazmat.2007.10.059